DEVELOPMENT OF COMPOSITE ELECTRODES CONTAINING GEOPOLYMER BINDER FOR ELECTROCHEMICAL APPLICATIONS

SAWITTA TRIAMTHAISONG[1], CHAIYAPUT KRUEHONG[1],
WIRAT JARERNBOON[2,4], VITTAYA AMORNKITBAMRUNG[2,4],
PRINYA CHINDAPRASIRT[3,5], KAEWTA JETSRISUPARB[1,5,*]

[1]Department of Chemical Engineering, Faculty of Engineering,
[2]Department of Physics, Faculty of Science,
[3]Department of Civil Engineering, Faculty of Engineering,
[4]Integrated Nanotechnology Research Center,
[5]Sustainable Infrastructure Research and Development Center,
Khon Kaen University, Khon Kaen, 40002, Thailand
*Corresponding Author: kaewta@kku.ac.th

Abstract

The requirements for electrode materials are high electronic conductivity, fast kinetics, high mechanical stability, and high chemical stability under oxidative and reductive environment. In this work, composite electrodes have been prepared containing geopolymer (made from Fly Ash (FA)), zinc, and Multiwalled Carbon Nanotubes (MWCNT) or graphite deposited on a nickel foam with different compositions (FA:Zn:MWCNT or FA:Zn:Graphite, mass ratio = 12:6:1 or 6:6:1). While the commercial zinc plate demonstrated clear oxidation and reduction reactions during cyclic voltammetry, no electrochemical reactions of zinc were observed with the composite electrodes. The composite electrodes suffered from high resistance, which could not be overcome even with reduced geopolymer content. The FE-SEM images indicated that the composite electrodes containing MWCNT were better dispersed than those containing graphite. Moreover, the composite electrode containing FA:Zn:MWCNT = 6:6:1 showed a lower overpotential for Oxygen Evolution Reaction (OER) compared to those with FA:Zn:Graphite at the same mass ratio. The surface morphology, homogeneity and chemical compositions lead to the change of the electrocatalyst activity towards OER. The electrode containing MWCNT may be attractive as anode for alkaline water electrolysis for hydrogen production. Further experiments should focus on optimization of the electrode composition to enhance its conductivity, activity and stability.

Keywords: Cyclic voltammetry, Geopolymer binder, Oxygen evolution reaction, Zinc electrode.

1.Introduction

Nowadays, the demand for safe, environmentally friendly, robust and reliable energy storage is continuously increasing due to the growing needs of renewable power generation to replace the use of depleting fossil fuels [1]. Although the technology of lithium-ion batteries is well established in mobile and stationary applications, lithium has a limited reserve and a high future demand has been forecasted [2]. From an industrial viewpoint, zinc batteries are of particular interest since these represent a safe, environmentally friendly, and potentially cost-effective alternative to the state-of-the-art lithium-ion batteries [3, 4].

Zinc as an electrode material has been extensively studied [5-8] and electrically rechargeable zinc electrode based batteries are developing [4]. However, zinc dissolution at high pH leads to a high self-discharge rate, limiting its use in many electrochemical applications [9]. Zinc is also applied as an electrocatalyst for the production of hydrogen by water splitting. Incorporation of zinc into the metal oxide catalyst shows an enhancement of the reactivity of Oxygen Evolution Reaction (OER) in alkaline electrolyzers [10, 11].

Electrodes can be produced in various sizes and shapes according to the applications. To ensure fast reaction kinetics, the active surface area is commonly enlarged by using (nano) powders. Binders are usually added to hold the electrode materials together and offer mechanical stability to the electrode. In addition, binders should facilitate electron and ion transfer to assist electrochemical reactions. Polymer materials such as PVDF, PVA and PTFE are commonly used as binders [3] due to their high chemical resistance, but their electronic insulation property leads to high electrode resistance. Alternatively, construction materials such as cement have been used for their high strength and the high alkalinity in the pore solution may aid the ion transport [12]. Yet, the production of cement is energy-intensive and cement industry is estimated to produce at least 5-7% of the CO_2 emission [13]. Geopolymer is seen as a potential alternative to cement [14]. During geopolymerization, dissolution of aluminosilicate with alkaline solution takes place leading to a network of geopolymer. The physical structure of geopolymer is a mostly amorphous gel with a small amount of crystalline zeolite formed during geopolymerization [15]. It has the strength comparable to the cement counterpart and can be produced from waste. In addition, the presence of the alkaline pore solution of the geopolymer can serve as an electrolyte (pH typically higher than 10) [16, 17]. Moreover, geopolymer possesses reasonable electrical conductivity of 1.5×10^{-6} S/cm at room temperature [18]. Therefore, geopolymer could be regarded as a potential binder for electrodes.

Carbonaceous materials such as graphite, acetylene black and carbon nanotubes are commonly used as additives to improve the electronic properties of materials [19, 20]. Incorporation of carbon nanotubes in geopolymer has proven to reduce the absolute value of impedance and feasibly increase the electron conductivity of the geopolymer [21].

The aim of this study was to investigate the potential use of geopolymer binder for zinc-based electrodes in electrochemical applications. Composite electrodes containing zinc, carbonaceous materials (MWCNT and graphite) and different geopolymer contents were prepared. The morphology and chemical composition of the composite electrodes were characterized by FE-SEM/EDX and XRD analyses and their electrochemical behaviour in 1 M KOH were studied by Cyclic

Voltammetry (CV). The result indicated that although zinc is distributed throughout the matrix, the high resistance of geopolymer may inhibit the formation of electronic percolation. The electrochemical behaviour of zinc was not observed, therefore the prepared electrodes may not be suitable for zinc anode battery. Nevertheless, the composite electrodes showed lower overpotential for the OER than that of zinc. The electrocatalyst activity of the electrode composites for OER is largely affected by the electrode composition. Such electrodes may find use as an anode in alkaline water electrolysis for hydrogen production.

2. Materials and Methods

2.1. Materials

Class *F* Fly Ash (FA) from Mae Moh Power Plant in Lampang province, Thailand was used as aluminosilicate source for geopolymer binder. Previously, Chindaprasirt et al. [22] reported the chemical composition of the fly ash. Sodium hydroxide (NaOH, 85% purity, ACI Labscan Limited, Thailand), sodium silicate (Na_2SiO_3, solution containing 12.0-12.8% Na_2O and 28.5-30.5% SiO_2, Wee-rin Chemical Limited Partnership, Thailand), zinc powder (99.9% purity, Ajax Finechem, Auckland, New Zealand) and Multi-Walled Carbon Nanotubes (MWCNT, >90% purity, 10 nm diameter, Nano generation, Thailand) were used as received. Commercial zinc plate (tested area 2 cm^2) was used as a control experiment in cyclic voltammetry. The purity of the zinc plate is 99.94% as determined by Optical Emission Spectrometer (ARL 3460 OES, Thermo Fischer Scientific).

2.2. Preparation of composite electrodes

The composite electrodes were prepared in one-pot as shown schematically in Fig. 1. The Fly Ash (FA) was mixed with zinc powder and MWCNT or graphite with the mass ratio of FA:Zn:MWCNT or FA:Zn:Graphite = 12:6:1 and 6:6:1. The FA was activated using 1 M NaOH and Na_2SiO_3 solution with the ratio of 6:4 (v/v), respectively. The ratio of FA to liquid was 12:10 (m/v). The electrode components were added as follows: First, the FA was mixed with 1 M NaOH and Na_2SiO_3 solution with FA:NaOH:Na_2SiO_3 = 12:5:3 (m/v/v) using a ceramic pestle. The liquid solution was added dropwise to form a smooth paste for 10 minutes. Second, graphite or MWCNT was added into the paste and mixed with the rest of NaOH and Na_2SiO_3 solution for two minutes. Third, zinc powder was added to the slurry and the mixing continued for 5 minutes till the paste thickened. Next, the electrode paste was cast on a nickel foam current collector (2 cm long × 1 cm wide) and left to set at room temperature overnight. Finally, the electrodes were cured at 65˚C in a closed plastic container in the presence of water for 3 hours. For the geopolymer electrode, the same sequence of preparation was applied without the addition of zinc powder and carbonaceous materials. The final deposited area was 2 cm^2 (1 cm × 1 cm, two-sided).

2.3. Material characterization

Powder X-Ray Diffraction (XRD) patterns were collected on a diffractometer (Model D8 Discover, Bruker AXS, Germany) using Cu Kα radiation with λ = 1.5418A, 40 kV and 44 mA, at a scan range of 20°-65° at room temperature and scan speed of 1° per min. The morphology and compositions of the cross-sectional

areas of various electrodes were studied using a Field Emission Scanning Electron Microscope (FE-SEM, Carl Zeiss Auriga) at an acceleration voltage of 3 kV.

2.4. Electrochemical characterization

Electrochemical characterization was carried out using a Gamry R600 potentiostat. Prior to the Cyclic Voltammetry (CV) experiments, the cell was conditioned under Open Circuit Voltage (OCV) to ensure constant voltage for at least 10 minutes using a two-point-probe cell with a nickel foam Counter Electrode (CE) and a commercial zinc plate or composite electrodes with geopolymer binder as Working Electrode (WE). Prior to use, the zinc plate was polished with sandpaper, rinsed with ethanol and sonicated in ethanol for 15 minutes to remove grease and contaminations on its surface.

The CV experiments employed a three-point-probe cell with a zinc plate or electrode composite WE, an Ag/AgCl in saturated KCl reference electrode (RE), and a nickel foam CE (Fig. 2). A Luggin capillary filled with KCl salt bridge was placed in the electrolyte near to the working electrode surface to minimize errors caused by iR drop. The electrolyte was 1 M KOH solution. A nickel foam was used as counter electrode. All experiments were carried out at room temperature with the scan rate of 10 mV/s. The current density (A/cm^2) is reported to eliminate the effects of geometrical surface area. In this way, different electrode materials can be compared.
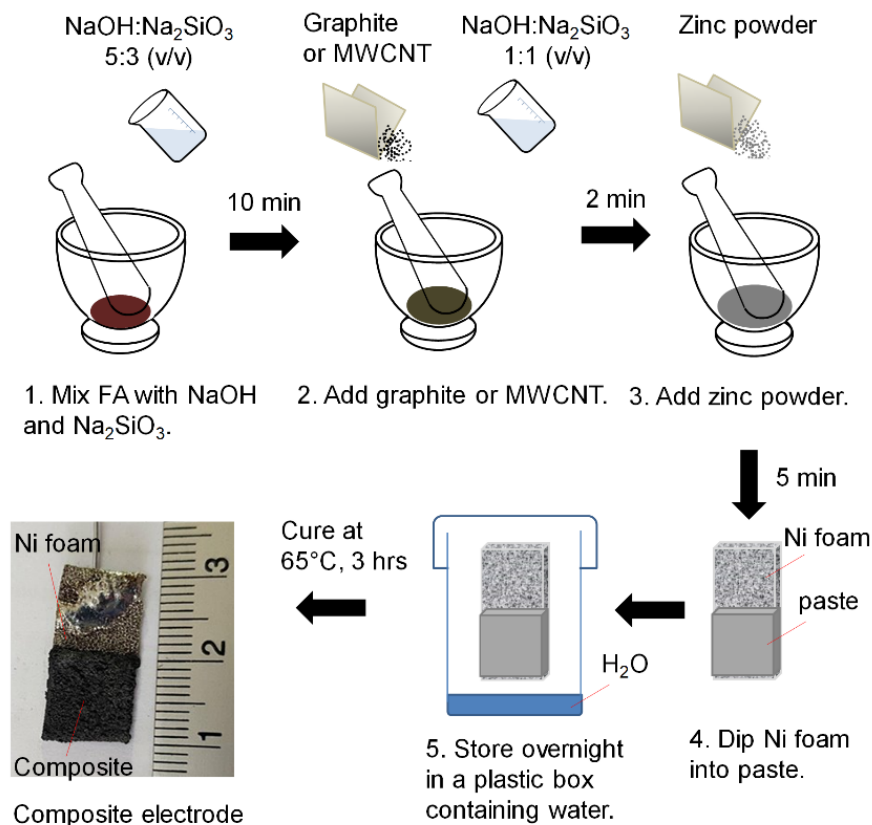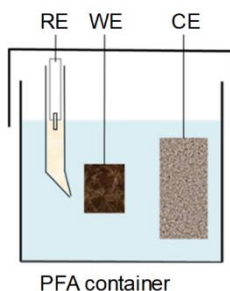

Fig. 1. Schematic representation of electrode preparation.

Fig. 2. Three-point probe configuration for cyclic voltammetry experiment with a nickel foam Counter Electrode (CE), Ag/AgCl in saturated KCl Reference Electrode (RE) and zinc plate or composite electrodes as Working Electrodes (WE). The electrolyte used in this study is 1 M KOH solution at room temperature.
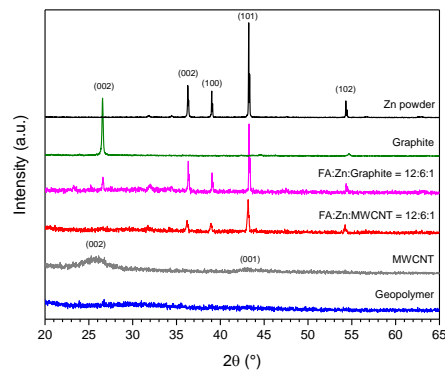
3. Results and Discussion

To investigate the crystallinity and composition of zinc, graphite, MWCNT, geopolymer and the as-prepared electrodes, XRD analysis was carried out as shown in Fig. 3. The geopolymer was amorphous as indicated by the absence of any crystalline peaks [23]. The XRD pattern of MWCNT shows characteristic peaks for the plane (002) and (101) at $2\theta = 25°$ and $43°$, respectively, confirming the nanocrystalline hexagonal structure of MWCNT [24]. When the MWCNTs are incorporated in the electrode paste containing the ratio of FA:Zn:MWCNT = 12:6:1, these peaks are not detected in the XRD pattern because of the low intensity. For graphite, a sharp peak at $2\theta = 27°$ relative to the plane (002) is found, indicating a crystalline structure [25]. This characteristic graphite peak is clearly seen in the FA:Zn:Graphite sample. The diffraction pattern of zinc powder shows prominent peaks at $2\theta = 36°, 39°, 43°$ and $54°$, which can be ascribed to the (002), (100), (101) and (102) planes, respectively [26]. These characteristic diffraction peaks can also be found when zinc is incorporated in the electrode composites (samples FA:Zn:Graphite and FA:Zn:MWCNT). It is likely that the composites may contain trace amounts of ZnO as indicated by small peaks at $2\theta = 32°$ and $34°$ [27]. ZnO could have been formed when zinc powder was exposed to the alkaline solution during electrode preparation. No other diffraction peaks were detected, indicating that no other crystalline species exist in the electrode composites.

FE-SEM/EDX analyses were carried out to investigate the morphology and confirm the distribution of elements present in the composite electrodes. As depicted in Fig. 4(a), the cross-sectional surface of the electrode with FA:Zn:MWCNT = 12:6:1 appears rough and is covered with MWCNT bundles and products of the geopolymerization reaction. Few rod-like crystal structures of gypsum imbedded in the matrix can be observed. In addition, the original sphere shape of undissolved FA is still visible. With a decrease in geopolymer content (FA:Zn: MWCNT = 6:6:1) the MWCNT bundles are denser and more agglomerated, likely because of the higher concentration (Fig. 4(b)). When MWCNT is replaced by micronsized graphite, various crystal sizes of graphite particles coexist in the geopolymer matrix as well as undissolved FA (Fig. 4(c)). Since the viscosity of the electrode paste rises with decreasing geopolymer content, mixing is less effective, resulting in a nonhomogeneous distribution of carbonaceous materials. A decrease in the

geopolymer content leads to the formation of graphite clusters (Fig. 4(d)). Thereby the utilization of graphite could be less effective and may eventually lower the conductivity. Although no specific structure is observed for zinc, the EDX analysis confirmed the presence of zinc and carbon throughout the matrix of each electrode composite (not shown). The insets symbolize the distribution of carbonaceous materials in the electrode matrix. The composite electrodes containing MWCNT (Figs. 4(a) and (b)) appear more homogeneous than those containing micron-sized graphite particles (Figs. 4(c) and (d)).

Figure 5 shows the voltammograms obtained in 1 M KOH using a scan rate of 10 mV/s. During the anodic sweep of the commercial zinc plate, a zinc stripping loop from -1.43 to -0.9 V is observed, as a result of the oxidation of zinc that causes a positive current flow. The shape of this zinc stripping loop is quite similar to zinc oxidation in a solution containing 2.34 M NH_4Cl and 0.51 M $ZnCl_2$ solution [9]. In alkaline solution, oxidation of zinc leads to zinc dissolution to form zincate complexions that dissolve in the alkaline electrolyte (Eqs. (1-2)). Cai and Park [28] reported that oxidation of zinc in 1 M KOH shows two prominent anodic peaks according to the formation of $Zn(OH)_4^{2-}$ and $Zn(OH)_3^{-}$. Once the concentration of zincate complex ions reaches saturation, a porous ZnO layer deposits on the zinc metal surface (Eq. (3)). This ZnO layer acts as an insulating layer as well as a barrier for electrolyte diffusion, and eventually stops oxidation of zinc, causing dramatic current drop [28]. This behaviour is characteristic for passivation of zinc. In the last step of the anodic sweep, oxygen gas is formed by oxidation of hydroxide ions when the potential applied on the electrode is more than 1.1 V (Eq. (4)).

$$Zn + 4OH^- \rightarrow Zn(OH)_4^{2-} + 2e^- \tag{1}$$

$$Zn + 3OH^- \rightarrow Zn(OH)_3^- + 2e^- \tag{2}$$

$$Zn(OH)_4^{2-} \rightarrow ZnO + H_2O + 2OH^- \tag{3}$$

$$4OH^- \rightarrow O_2 + 2H_2O + 4e^- \tag{4}$$

Fig. 3 XRD patterns of electrode composites containing ratios of FA:Zn:MWCNT and FA:Zn:Graphite = 12:6:1 compared to starting materials (geopolymer, MWCNT, graphite, and zinc powder). Peak intensities for graphite and Zn powder were scaled down 10 times for better comparison.

(a) FA:Zn:MWCNT = 12:6:1. **(b) FA:Zn:MWCNT = 6:6:1.**

(c) FA:Zn:Graphite = 12:6:1. **(d) FA:Zn:Graphite = 6:6:1.**
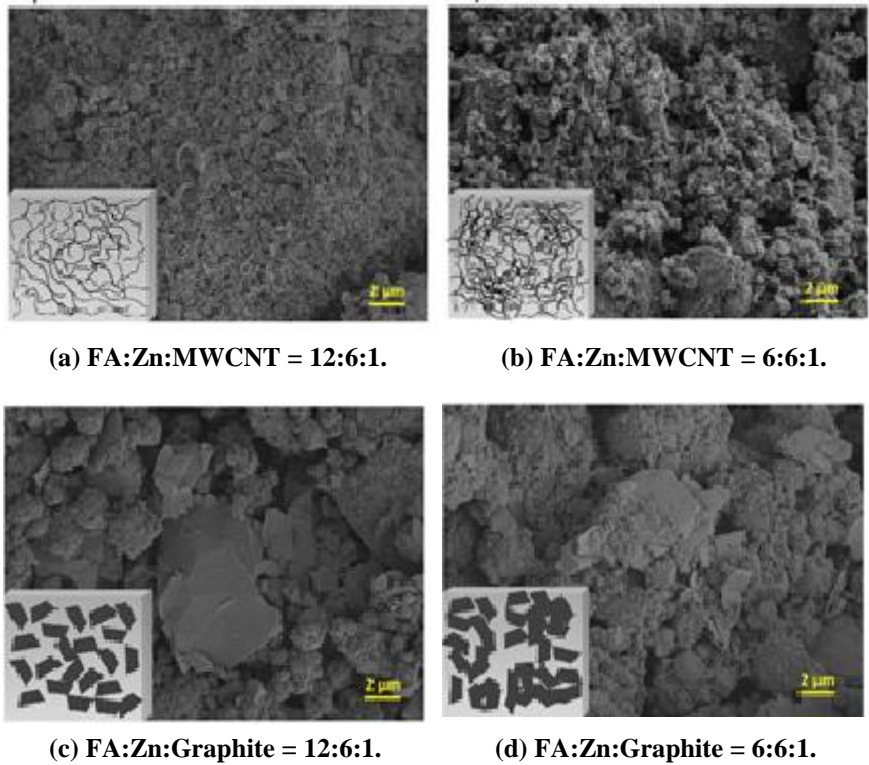
Fig. 4. Cross-sectional FE-SEM images of electrode composites containing FA:Zn:MWCNT with mass ratios of (a) 12:6:1 and (b) 6:6:1, and composites containing FA:Zn:Graphite with mass ratios of (c) 12:6:1 and (d) 6:6:1. Figure insets are schematic representations of carbonaceous materials (MWCNT and graphite) distribution in the composites.
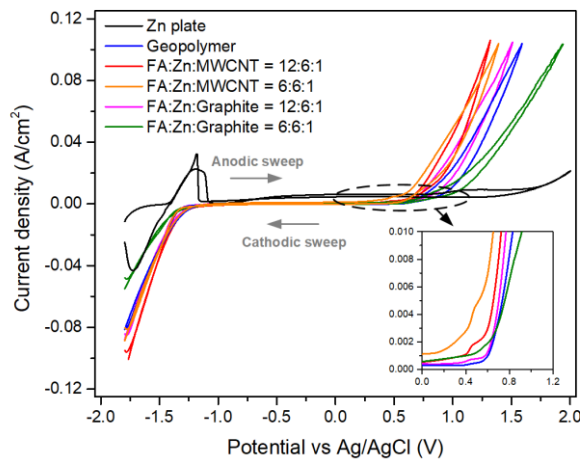
Fig. 5. Cyclic voltammograms of composite electrodes in 1 M KOH with a scan rate of 10 mV/s. The inset figure presents the overpotentials at 10 mA/ cm^2 measured during anodic sweep.

During the cathodic sweep, a second anodic peak is observed at -1.1 V, indicating that the insulating ZnO layer is dissolved in alkaline solution and removed from the surface. Zinc is then exposed to the electrolyte and oxidation can further take place. This emphasizes the difficulties of alkaline zinc batteries since the dissolution of the passive film leads to capacity loss and shortens the battery lifetime [28]. Oxidation during the cathodic sweep, however, has not been observed in neutral electrolyte [9], implying that dissolution of oxidation products is higher in alkaline electrolyte than in neutral electrolyte.

The zinc reduction loop starts at -1.42 V. The amplitude of current generated in the cathodic loop is comparable to the sum of oxidation peaks. The difference could be due to the diffusion of zinc oxidation products away from the electrode. Thus, the zinc plate is not fully rechargeable if the ions migrate away from the electrode. To improve the electrode lifetime and capacity, the electrode could be designed to restriction motion. Different methods have been applied, for example, incorporation of structured materials such as activated carbon [5] in the electrode to accommodate the ions during oxidation.

In the presence of geopolymer binder, the voltammograms of composite electrodes containing zinc and carbonaceous materials (FA:Zn:MWCNT and FA:Zn:Graphite) are similar to that of the geopolymer electrode (Fig. 5). Despite the presence of zinc powder in the composite electrodes, no current response associated with zinc oxidation is observed. Since the geopolymer could potentially lead to high electrode resistance, reduction of binder content by half (FA:Zn:MWCNT or graphite of 6:6:1) has been investigated, yet the same trend is obtained. The result implies that the insulating property of geopolymer inhibited the reaction kinetics of active zinc in the electrodes. Although the FE-SEM/EDX analyses show the distribution of zinc and carbon throughout the electrode matrix (Fig. 4), the formation of a conductive path may not be completed. Further reduction in the binder content may help to form electronic percolation however the mechanical stability will be lower. We found that the composite electrodes with mass ratio FA:Zn:MWCNT or graphite of 6:6:1 have a low mechanical stability.

The oxidation of hydroxide ions to oxygen (Eq. (4)) of all electrode composites takes place at lower than 0.6 V, which is considerably lower than that of zinc plate (>1 V). Such lowering of the voltage required for oxidation of hydroxyl ions to oxygen could be beneficial for hydrogen production by water electrolysis because the sluggish kinetics of the oxygen evolution is the bottleneck of polymer electrolyte membrane electrolyzers [29]. Nickel-based electrodes are well-known to have a catalytic activity in OER [30-32] and nickel foam is considered a suitable substrate for electrocatalyst loading due to its high surface area [11]. The presence of nickel foam as a current collector of the composite electrodes might as well play a role in lowering the oxidation potential.

The overpotential is one of the electrocatalytic kinetic parameters used to evaluate the performance of electrocatalysts. A low overpotential is preferred since it indicates a low activation energy, implying superior electrocatalytic ability [11]. The inset of Fig. 5 and the data in Table 1 show the overpotential at 10 mA/cm^2 at room temperature and 1 M KOH. The protocol developed by McCrory et al. [33] conditions are slightly different since 1 M KOH was used instead of NaOH [11].

Table 1. Comparison of the overpotentials vs Ag/AgCl of various composite electrodes measured during anodic sweep at 10 mA/cm² in 1 M KOH at room temperature, and composite loading on a nickel foam current collector.

	Overpotential (mV) at 10 mA/cm²	Loading (g/cm²)
Geopolymer	830	0.17
FA:Zn:MWCNT = 12:6:1	724	0.25
FA:Zn:MWCNT = 6:6:1	650	0.20
FA:Zn:Graphite = 12:6:1	768	0.19
FA:Zn:Graphite = 6:6:1	914	0.32

The overpotentials of composite electrodes containing FA:Zn:MWCNT and FA:Zn:Graphite of 12:6:1 is slightly lower than that of the geopolymer electrode, implying better electrocatalytic performance. For these samples, only small effects of MWCNT or graphite were observed at this mass ratio, which may indicate the high amount of geopolymer predominates the electrochemical property of the composite electrodes. When reducing the geopolymer content, the composite electrode containing mass ratios FA:Zn:MWCNT of 6:6:1 shows the lowest overpotential (650 mV at 10 mA/cm²) for OER compared to the other electrodes, while the electrode with mass ratio of FA:Zn:Graphite = 6:6:1, however, shows an inferior OER performance. Dubey et al. [34], is found to be in good agreement with the result. They reported that MWCNT has a superior activity towards OER over graphite because the hydroxide ions react with defects (displacement or absence of carbon atoms) in MWCNT, facilitating the dissociation reaction of hydroxide to oxygen [34]. Moreover, the FE-SEM image of FA:Zn:Graphite = 6:6:1 indicates that the graphite is poorly dispersed (Fig. 4(d)). These results may imply that the activity of OER is largely affected by the electrode composition (i.e., graphite versus MWCNT) as well as homogeneity of the samples. Although the overpotentials found for the composite electrodes are still high compared to typical noble metal and metal oxide electrocatalysts for OER [11, 33], the electrochemical property and morphology of composite electrodes using geopolymer binder can be tailored for further improvements.

4. Conclusions

Electrode composites have been prepared to contain geopolymer, zinc, and carbonaceous material (MWCNT or graphite) deposited on a nickel foam current collector. The electrochemical behaviour of composite electrodes containing geopolymer strongly depends on the electrode composition (fly ash content and carbonaceous material). During cyclic voltammetry, the commercial zinc plate shows a pronounced oxidation and reduction, while no electrochemical reactions of zinc are observed with the composite electrodes. This is likely due to the high resistance of the composite: when binder (in this case geopolymer) is present, the resistance of the electrode increases and predominates the electrochemical properties of zinc. The prepared electrodes might not be suitable for zinc anode batteries. Even though no zinc reactivity was seen, the composites containing MWCNT were better dispersed than those containing graphite (as evidenced by FE-SEM). In addition, the electrode composite containing MWCNT at the mass ratios of FA:Zn:MWCNT = 6:6:1 showed a lower overpotential for OER than its graphite counterpart during the anodic sweep, indicating that these materials could be used as anodes for alkaline water electrolysis for hydrogen production. Therefore, geopolymer could be considered an interesting

material of choice as electrode binder for OER electrocatalysts. Further tests should be conducted to establish the feasibility of the geopolymer composite electrodes.

Acknowledgement

Greek Symbols

θ	Diffraction angle (Fig. 3), deg.
λ	Radiation wavelength, nm

Abbreviations

CE	Counter Electrode
CV	Cyclic Voltammetry
EDX	Energy Dispersive X-Ray Spectroscopy
FA	Fly Ash
FE-SEM	Field Emission Scanning Electron Microscopy
OCV	Open Circuit Voltage
OER	Oxygen Evolution Reaction
OES	Optical Emission Spectrometer
PFA	Perfluoroalkoxy Alkane
PTFE	Polytetrafluoroethylene
PVA	Polyvinyl Alcohol
PVDF	Polyvinylidene Fluoride
RE	Reference Electrode
WE	Working Electrode
XRD	X-Ray Diffraction

References

1. Gyuk, I.; Johnson, M.; Vetrano, J.; Lynn, K.; Parks, W.; Handa, R.; Kannberg, L.; Hearne, S.; Waldrip, K.; and Braccio, R. (2013). Grid energy storage. *US Department of Energy*.

2. Peiro, L.T.; Villalba Mendez, G.B.; and Ayres, R.U. (2013). Lithium: Sources, production, uses, and recovery outlook. *Journal of the Minerals, Metals & Materials Society*, 65(8), 986-996.

3. Mainar, A.R.; Colmenares, L.C.; Blazquez, J.A.; and Urdampilleta, I. (2018). A brief overview of secondary zinc anode development: The key of improving zinc-based energy storage systems. *International Journal of Energy Research*, 42(3), 903-918.

4. Linden, D.; and Reddy, T.B. (2002). *Handbook of batteries* (3rd ed.). New York: McGraw Hill.

5. Li, H.; Xu, C.; Han, C.; Chen, Y.; Wei, C.; Li, B.; and Kang, F. (2015). Enhancement on cycle performance of Zn anodes by activated carbon

modification for neutral rechargeable zinc ion batteries. *Journal of the Electrochemical Society*, 162(8), A1439-A1444.

6. Zhang, X.G. (2006). Fibrous zinc anodes for high power batteries. *Journal of Power Sources*, 163(1), 591-597.

7. Zhang, N.; Cheng, F.; Liu, J.; Wang, L.; Long, X.; Liu, X.; Li, F.; and Chen, J. (2017). Rechargeable aqueous zinc-manganese dioxide batteries with high energy and power densities. *Nature Communications*, 8, Article No. 405.

8. Parker, J.F.; Chervin, C.N.; Nelson, E.S.; Rolison, D.R.; and Long, J.W. (2014). Wiring zinc in three dimensions re-writes battery performance-dendrite-free cycling. *Energy and Environmental Science*, 7(3), 1117-1124.

9. Thomas Goh, F.W.; Liu, Z.; Andy Hor, T.S.; Zhang, J.; Ge, X.; Zong, Y.; Yu, A.; and Khoo, W. (2014). A near-neutral chloride electrolyte for electrically rechargeable zinc-air batteries. *Journal of the Electrochemical Society*, 161(14), A2080-A2086.

10. Liu, X.; Chang, Z.; Luo, L.; Xu, T.; Lei, X.; Liu, J.; and Sun, X. (2014). Hierarchical $Zn_xCo_{3-x}O_4$ nanoarrays with high activity for electrocatalytic oxygen evolution. *Chemistry of Materials*, 26(5), 1889-1895.

11. Suen, N.-T.; Hung, S.-F.; Quan, Q.; Zhang, N.; Xu, Y.-J.; and Chen, H.M. (2017). Electrocatalysis for the oxygen evolution reaction: Recent development and future perspectives. *Chemical Society Reviews*, 46(2), 337-365.

12. Meng, Q.; and Chung, D.D.L. (2010). Battery in the form of a cement-matrix composite. *Cement and Concrete Composites*, 32(10), 829-839.

13. McLellan, B.C.; Williams, R.P.; Lay, J.; van Riessen, A.; and Corder, G.D. (2011). Costs and carbon emissions for geopolymer pastes in comparison to ordinary portland cement. *Journal of Cleaner Production*, 19(9-10), 1080-1090.

14. Srinivasan, K.; and Sivakumar, A. (2013). Geopolymer binders: A need for future concrete construction. *ISRN Polymer Science*, Article ID509185, 8 pages.

15. Provis, J.L.; Lukey, G.C.; and Van Deventer, J.S.J. (2005). Do geopolymers actually contain nanocrystalline zeolites? A reexamination of existing results. *Chemistry of Materials*, 17(12), 3075-3085.

16. Lloyd, R.R.; Provis, J.L.; and Van Deventer, J.S.J. (2010). Pore solution composition and alkali diffusion in organic polymer cement. *Cement and Concrete Research*, 40(9), 1386-1392.

17. Cyr, M.; and Pouhet, R. (2016). Carbonation in the pore solution of metakaolin-based geopolymer. *Cement and Concrete Research*, 88, 227-235.

18. Cui, C.M.; Zheng, G.J.; Han, Y.C.; Su, F.; and Zhou, J. (2008). A study on electrical conductivity of chemosynthetic Al_2O_3-$2SiO_2$ geoploymer materials. *Journal of Power Sources*, 184(2), 652-656.

19. Payakaniti, P.; Pinitsoontorn, S.; Thongbai, P.; Amornkitbamrung, V.; and Chindaprasirt, P. (2017). Electrical conductivity and compressive strength of carbon fiber reinforced fly ash geopolymeric composites. *Construction and Building Materials*, 135, 164-176.

20. Marinho, B.; Ghislandi, M.; Tkalya, E.; Koning, C.E.; and de With, G. (2012). Electrical conductivity of compacts of graphene, multi-wall carbon nanotubes, carbon black, and graphite powder. *Powder Technology*, 221, 351-358.

21. Kusak, I.; Lunak, M.; and Rovnanik, P. (2016). Electric conductivity changes in geopolymer samples with added carbon nanotubes. *Procedia Engineering*, 151, 157-161.

22. Chindaprasirt, P.; Jaturapitakkul, C.; and Sinsiri, T. (2007). Effect of fly ash fineness on microstructure of blended cement paste. *Construction and Building Materials*, 21(7), 1534-1541.

23. Somna, K.; Jaturapitakkul, C.; Kajitvichyanukul, P.; and Chindaprasirt, P. (2011). NaOH-activated ground fly ash geopolymer cured at ambient temperature. *Fuel*, 90(6), 2118-2124.

24. Hsu, Y.-W.; Wu, C.-C.; Wu, S.-M.; and Su, C.-C. (2017). Synthesis and properties of carbon nanotube-grafted silica nanoarchitecture-reinforced poly (lactic acid). *Materials (Basel)*, 10(7), PMC5551872.

25. Zhang, K.; Zhang, Y.; and Wang, S. (2013). Enhancing thermoelectric properties of organic composites through hierarchical nanostructures. *Scientific Reports*, 3, Article No. 3448.

26. Li, H.F.; Xie, X.H.; Zheng, Y.F.; Cong, Y.; Zhou, F.Y.; Qiu, K.J.; Wang, X.; Chen, S.H.; Huang, L.; Tian, L.; and Qin, L. (2015). Development of biodegradable Zn-1X binary alloys with nutrient alloying elements Mg, Ca and Sr. *Scientific Reports*, 5, Article No. 10719.

27. Knijnenburg, J.T.N.; Hilty, F.M.; Krumeich, F.; Zimmermann, M.B.; and Pratsinis, S.E. (2013). Multimineral nutritional supplements in a nano-CaO matrix. *Journal of Materials Research*, 28(8), 1129-1138.

28. Cai, M.; and Park, S.-M. (1996). Spectroelectrochemical studies on dissolution and passivation of zinc electrodes in alkaline solutions. *Journal of the Electrochemical Society*, 143(7), 2125-2131.

29. Sapountzi, F.M.; Gracia, J.M.; Weststrate, C.J.K.J.; Fredriksson, H.O.A.; and Niemantsverdriet, J.W.H. (2017). Electrocatalysts for the generation of hydrogen, oxygen and synthesis gas. *Progress in Energy and Combustion Science*, 58, 1-35.

30. Perez-Alonso, F.J.; Adan, C.; Rojas, S.; Pena, M.A.; and Fierro, J.L.G. (2014). Ni/Fe electrodes prepared by electrodeposition method over different substrates for oxygen evolution reaction in alkaline medium. *International Journal of Hydrogen Energy*, 39(10), 5204-5212.

31. Seetharaman, S.; Balaji, R.; Ramya, K.; Dhathathreyan, K.S.; and Velan, M. (2014). Electrochemical behaviour of nickel-based electrodes for oxygen evolution reaction in alkaline water electrolysis. *Ionics*, 20(5), 713-720.

32. Fabbri, E.; Habereder, A.; Waltar, K.; Kotz, R.; and Schmidt, T.J. (2014). Developments and perspectives of oxide-based catalysts for the oxygen evolution reaction. *Catalysis Science and Technology*, 4(11), 3800-3821.

33. McCrory, C.C.L.; Jung, S.; Ferrer, I.M.; Chatman, S.M.; Peters, J.C.; and Jaramillo, T.F. (2015). Benchmarking hydrogen evolving reaction and oxygen evolving reaction electrocatalysts for solar water splitting devices. *Journal of the American Chemical Society*, 137(13), 4347-4357.

34. Dubey, P.K.; Sinha, A.S.K.; Talapatra, S.; Koratkar, N.; Ajayan, P.M.; and Srivastava, O.N. (2010). Hydrogen generation by water electrolysis using carbon nanotube anode. *International Journal of Hydrogen Energy*, 35(9), 3945-3950.